Analysis of recombinant tagged equilibrative nucleoside transporter 1 (ENT1) expressed in *E. coli*[1]

German Reyes, Nicole M.I. Nivillac, Maria Chalsev, and Imogen R. Coe

Abstract: Nucleoside transporters (NTs) are integral membrane proteins necessary for the cellular entry of nucleoside analog drugs used in chemotherapeutic treatment of conditions such as cancer and viral or parasitic infections. NTs are also the targets of certain drugs used in the treatment of various cardiovascular conditions. Because of the importance of NTs in drug uptake, determination of the three-dimensional structure of these proteins, particularly hENT1, has the potential to improve these treatments through structure-based design of more specifically targeted and transported drugs. In this paper, we use NMR spectroscopy to investigate the structure of the large intracellular loop between transmembrane domains 6 and 7 and we also describe a method for the successful overexpression of full-length hENT1 in a bacterial system. Recombinant tandem histidine-affinity (HAT) and 3×FLAG tagged hENT1 was overexpressed in *E. coli*, affinity purified, and functionally characterized by nitrobenzylthioinosine (NBTI) binding. Anti-3×FLAG immunodetection confirmed the expression of N-HAT-3×FLAG-hENT1, while increased NBTI binding (3.2-fold compared with controls) confirmed the conformational integrity of the recombinant hENT1 within the bacterial inner membrane. Yields of recombinant hENT1 using this approach were ∼15 µg/L of bacterial culture and this approach provides a basis for large-scale production of protein for a variety of purposes.

Key words: hENT1, structure, recombinant, overexpression, bacteria.

Résumé : Les transporteurs de nucléosides (TN) consistent en protéines membranaires intégrales nécessaires à l'entrée dans les cellules d'analogues des nucléosides utilisés en chimiothérapie pour traiter des maladies ou des situations comme le cancer ou les infections virales/parasitaires. Les TN sont aussi les cibles de certains médicaments utilisés dans le traitement de certaines maladies cardiovasculaires. À cause de l'importance des TN dans la capture de médicaments, la détermination de la structure tridimensionnelle de ces protéines, particulièrement hENT1, pourrait permettre d'améliorer ces traitements par la conception, d'après cette structure, de médicaments ciblés et transportés de manière plus spécifique. Dans cet article, nous utilisons la spectroscopie RMN afin d'examiner la structure de la grande boucle intracellulaire située entre les domaines 6 et 7, et nous décrivons aussi une méthode efficace de surexpression de hENT1 de pleine longueur dans un système bactérien. Un transporteur hENT1 recombinant portant des étiquettes d'affinité d'histidine en tandem (HAT) et 3×FLAG a été surexprimé chez *E. coli*, purifié par affinité et caractérisé fonctionnellement par la liaison de nitrobenzylthioionsine (NBTI). La détection immunologique à l'aide d'un anti-3×FLAG a confirmé l'expression de N-HAT-3×FLAG-hENT1, alors que l'augmentation de la liaison de NBTI (3,2 fois comparativement au contrôle) a confirmé l'intégrité conformationnelle du hENT1 recombinant au sein de la membrane interne bactérienne. La récolte de hENT1 recombinant était d'environ 15 µg/L de culture bactérienne en utilisant cette approche, celle-ci constituant une base à partir de laquelle la production à grande échelle de la protéine sera envisagée à différentes fins.

Mots-clés : hENT1, structure, recombinant, surexpression, bactérie.

[Traduit par la Rédaction]

Introduction

Structural characterization of proteins, especially those involved in cellular drug processing, has greatly increased in recent years, allowing more advanced structure-based drug design (Congreve et al. 2005; Blundell et al. 2006). Cytosolic drug-processing proteins are readily analyzed owing to their soluble nature, resulting in significant increases in the number of solved crystal structures in the Protein Data Bank (PDB, http://www.rcsb.org/pdb/home.do), while integral membrane protein (IMP) drug transporters have proved to be considerably more challenging to characterize owing to their hydrophobicity, labile nature, and low natural expression levels (Granseth et al. 2007; Lacapère et al. 2007; Reithmeier 2007). Prokaryotic homologs of mammalian

IMPs have proved useful in elucidating structures, since large quantities of high-quality protein can be produced, but for families such as the SLC29 (or ENT) family, where no prokaryotic homolog exists, limited structural information has been obtained.

Equilibrative nucleoside transporters (ENTs) are the entry portals in membranes for nucleosides and nucleobases, which have various biological functions (Löffler et al. 2007; Rose and Coe 2008; Young et al. 2008). However, there is much interest in the three-dimensional structure of ENTs because of their clinical relevance as nucleoside analog (NA) drug transporters. Nucleoside transporters (particularly ENT1 and CNT3) transport NA drugs that are used in the treatment of cancer (e.g., leukemias and solid tumors), viral infections (e.g., HIV and hepatitis B), and parasitic infections such as toxoplasmosis, malaria, and African sleeping sickness (King et al. 2006; Young et al. 2008). In addition, ENTs are targets for drugs used to treat certain neurovascular or cardiovascular conditions (Noji et al. 2004; King et al. 2006). ENT1 is ubiquitously expressed in human tissues and is responsible for a significant proportion of NA drug uptake (King et al. 2006). Many studies have led to a widely accepted two-dimensional topological model of ENTs that describes regions involved in substrate transport and residues important for substrate and drug binding (Young et al. 2008). In addition, advances in computational homology modeling have led to hypothetical three-dimensional models of ENTs that, along with the putative translocation sites, are in pressing need of validation through detailed structural studies as provided by NMR spectroscopy and X-ray crystallography (Young et al. 2008). Since the large intracellular loop of ENT1 has been hypothesized to be a site of regulatory interactions, we determined whether this region of ENT1 has defined structure, as predicted by protein structure prediction programs, using NMR. For more extensive structural analysis, large quantities of protein are needed and various approaches for producing large quantities of high-quality functional ENT protein have been investigated, including using mammalian, yeast, and insect host systems to overexpress recombinant ENTs (Vickers et al. 1999; Reyes et al. 2010; G. Reyes and I.R. Coe, unpublished data). However, we have found that these approaches are not optimal for the generation of the protein yields required for structural studies using X-ray and electron crystallography. As a result, we have developed a bacterial overexpression system that produces recombinant human ENT1 (hENT1) possessing correct ligand-binding conformation. Moreover, we propose that this approach can be scaled up to produce sufficient quantities of protein for crystallographic structural analysis.

Methods and materials

Construct design

The construct pN-HAT-3×FLAG-hENT1 was used for bacterial overexpression and consists of 3×FLAG-tagged hENT1 cDNA (Reyes et al. 2010) inserted into the vector pHAT20 (Clontech, Mountain View, California) between the *Hpa*I and *Kpn*I restriction sites. The primers used to PCR-amplify cDNA were sense primer, 5′-AGCTTTGT-TAAC*ATGGACTACAAAGACCATGACGGTGATTAT*-3′, and antisense primer, 5′-CGGGGTACC*TCACACAATTGCCCG-GAA*-3′ (restriction sites are underlined and protein-coding segments are italicized). The resultant construct encodes an amino-terminal double-tagged hENT1 protein under "slow" constitutive *lac* promoter control. Expression is inducible with 1 mmol/L isopropyl β-D-1-thiogalactopyranoside (IPTG). The HAT (histidine affinity tag) is upstream of the 3×FLAG tag (Sigma, St. Louis, Missouri) and can be removed with enterokinase treatment. Generation of a topological model of N-HAT-3×FLAG-hENT1 was aided by transmembrane domain assignments conducted with the shareware program TMpred (http://www.ch.embnet.org/software/TMPRED_form.html; Hofmann and Stoffel 1993), while secondary structure predictions and sequence analysis of the large intracellular loop of hENT1 and mENT1 were done using the programs PSIPRED (http://bioinf.cs.ucl.ac.uk/psipred; Bryson et al. 2005), ProtScale, following the Zimmerman amino acid scale (http://expasy.org/cgi-bin/protscale.pl; Gasteiger et al. 2005), and ClustalW2 (http://www.ebi.ac.uk/Tools/clustalw2/index.html; Chenna et al. 2003).

Protein overexpression

Bacterial overexpression of recombinant hENT1 was initiated by heat shock transformation of competent *E. coli* BL21(DE3) cells (EMD, Darmstadt, Germany) with the construct pN-HAT-3×FLAG-hENT1 and selection of positive colonies on ampicillin-supplemented LB plates (Amp, 50 μg/mL; Sigma). These plates were routinely used within 2 weeks (having been stored at 4 °C), as we noted that overexpression of recombinant hENT1 is unreliable after more than 14 days. Positive colonies were amplified by inoculating selective LB medium (50 μg/mL Amp) in shake flasks (volumes ≤ 50 mL) and incubating cultures at various temperatures (37 °C, 25 °C, and 20 °C) until culture densities reached OD_{600} values of 0.4 (16–48 h, 250 rpm), at which point the cultures were induced for 3–5 h with 1 mmol/L IPTG. Overexpression of N-HAT-3×FLAG-hENT1 was confirmed by anti-3×FLAG immunodetection (Sigma) on 1 mL aliquots of these bacterial cultures (suspended in standard 1× protein loading buffer [PLB: 62.5 mmol/L Tris–HCl pH 6.8, 2% (*v/v*) SDS, 5% (*v/v*) glycerol, 0.1 mol/L dithiothreitol (DTT), 0.03 mmol/L bromphenol blue] and heated at 85 °C for 10 min). Bacterial cells in the remaining culture were then pelleted by centrifugation (8000*g*, 20 min, 4 °C) and stored at –80 °C until further analysis, which was typically conducted within 2 weeks. Large-scale trial cultures (1 L) were grown in 1 L fermentors set at 20–22 °C, pH 7.0, 300 rpm, and >30% dissolved O_2. A non-induced overnight starter culture (100 mL) was used to inoculate the 1 L of selective LB (50 μg/mL Amp) and this culture was grown to a cell density of $OD_{600} \approx 1.6$, followed by induction with 1 mmol/L IPTG for 5 h.

Isolation of inner membranes from N-HAT-3×FLAG-hENT1 transformed bacterial cells was conducted following a previously described sucrose gradient method (Kotarski and Salyers 1984). Inner membranes were suspended in HEPES buffer (10 mmol/L, pH 7.4) and the presence of 3×FLAG-hENT1 was confirmed by anti-3×FLAG immunodetection.

NBTI binding assay

NBTI binding assays were conducted as previously described (Reyes et al. 2010) with a few modifications, on non-treated and osmotically shocked transformed bacterial cells. Modifications include incubating samples with increasing concentrations of [^{3}H]NBTI (0.1–15 nmol/L) and filtering the samples through Durapore membrane filters (0.22 μm, Millipore, Billerica, Massachusetts). Bacterial cells were osmotically shocked, following a standard procedure (Neu and Heppel 1965), to ensure accessibility of NBTI to the inner membrane, since the outer membrane of *E. coli* is impermeable to NBTI.

Tandem affinity purification

Total solubilized cell lysates used for the tandem purification were prepared by suspending the cell pellet in ice-cold lysis buffer pH 7.4 (50 mmol/L Tris–HCl, 150 mmol/L NaCl, 0.25% (*v/v*) Fos-Choline-12 (Anatrace, Maumee, Ohio), and EDTA-free protease inhibitors (Roche, Laval, Quebec); 10 mL/g of pellet) and disrupting the cells by probe sonication on ice (30% intensity, 4 cycles of 10–30 s, depending on aliquot volume). This greyish, more translucent solution was then allowed to mix with rotation for 2 h on ice (0 °C) to ensure full solubilization of membrane proteins while minimizing degradation. After this incubation, the solution was centrifuged (15 000*g*, 4 °C) to remove insoluble debris (in the pellet) and the remaining supernatant (total solubilized cell lysate) was used immediately to affinity purify the recombinant hENT1. Total protein content was determined using a reducing agent and detergent compatible (*RC DC*) Lowry assay (Bio-Rad, Mississauga, Ontario).

The isolation of N-HAT-3×FLAG-hENT1 from large-scale trials (1 L fermentor cultures) used a 4 mL Ni^{2+}-NTA column with a flow rate of 1 mL/min. Total solubilized cell lysates, as prepared above, were syringe filtered (0.45 μm; Millipore) and recirculated on the column overnight (0–4 °C). This was followed by washing with 100 mL of lysis buffer pH 7.4 and elution with 30 mL of lysis buffer supplemented with 100 mmol/L imidazole. The eluate was immediately bound to 200 μL of anti-3×FLAG M2 agarose resin and incubated overnight with rotation (4 °C). The resin was washed with 10 mL of ice-cold lysis buffer pH 7.4 (3 cycles, 15 min, 4 °C) and the elution fraction was collected using 150 μL of a modified 1× protein loading buffer [PLB*: 62.5 mmol/L Tris–HCl pH 6.8, 2% (*v/v*) SDS, 10% (*v/v*) glycerol]. PLB* differs from PLB in that it lacks DTT (reducing agent) and bromphenol blue (dye) to help minimize the displacement of IgG from the resin and to avoid interference by the buffer in subsequent *RC DC* Lowry assays. The presence of N-HAT-3×FLAG-hENT1 was confirmed using previously described methods (Reyes et al. 2010) including 10% SDS–PAGE with visualization by Bio-Safe Coomassie blue staining (detection range of 8–28 ng; Bio-Rad) and anti-3×FLAG immunodetection (1:30 000 antibody dilution). Band sizes and yields were estimated using a broad-range marker (7–175 kDa; New England Biolabs, Ipswich, Massachusetts) and BSA standards (1 μg/lane).

NMR spectroscopy

Two chimeric genes consisting of 6×His–ubiquitin, an intervening thrombin site, and residues 228–290 of hENT1 or mENT1 (large intracellular loops) were codon optimized and synthesized commercially (DNA2.0, Menlo Park, California) and inserted into the vector pJexpress 401.

The 6×His–ubiquitin–ENT1 (Ubq–ENT1) fusion peptides were expressed from a 1 L culture of *E. coli* BL21(DE3) in a minimum medium containing [^{15}N]ammonium chloride as the sole nitrogen source. Purification of the fusion peptides from the soluble fraction was achieved by nickel affinity and gel filtration chromatography. A sample of Ubq–ENT1 was prepared for NMR spectroscopy at a concentration of 0.2 mmol/L in 10 mmol/L sodium phosphate, pH 7.8, 150 mmol/L NaCl, and 0.05% sodium azide.

^{15}N-edited heteronuclear single-quantum coherence spectra (768 × 80 points) were acquired on a 600 MHz Varian NMR spectrometer equipped with a salt-tolerant cryogenic probe. The Ubq–ENT1 spectra were compared with the spectrum of a 6×His–ubiquitin fusion peptide (Ubq–PirB) containing an unrelated 36 amino acid sequence from human paired immunoglobulin-like receptor B (PirB). Spectra were processed with NMRPipe (Delaglio et al. 1995) and interpreted with NMR View (Johnson and Blevins 1994).
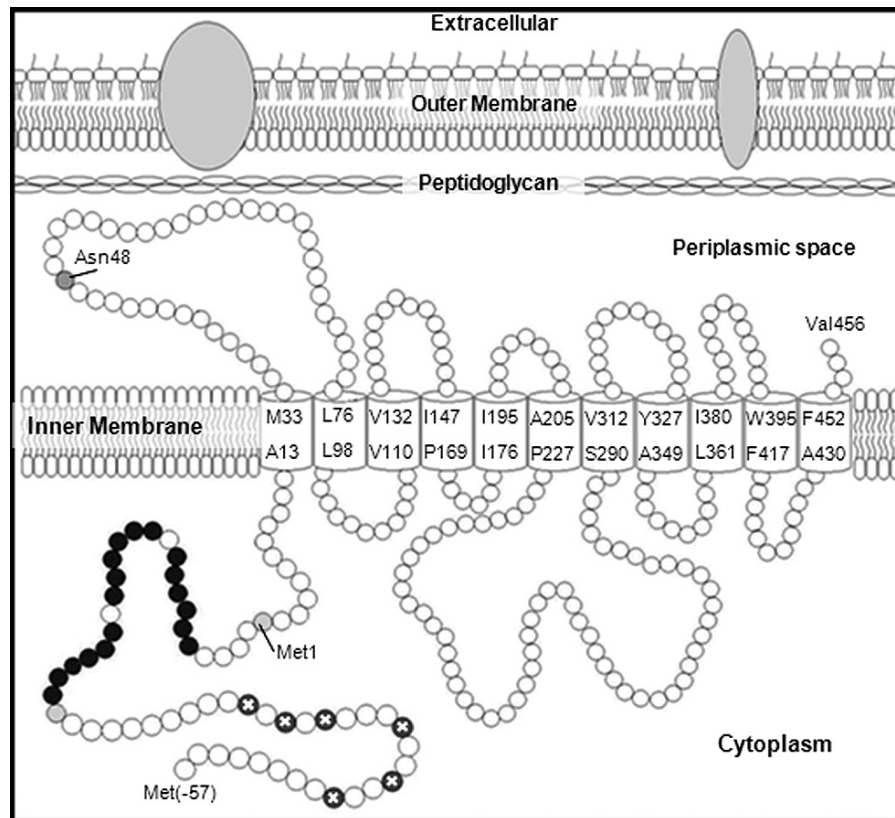
Results and discussion

Protein overexpression

This is the first report, to our knowledge, of the successful expression of recombinant hENT1 (N-HAT-3×FLAG-hENT1) in a bacterial host. This is a significant step towards three-dimensional analysis of hENT1, a clinically important drug transporter, because it represents an important step towards overcoming the problem of low yields of mammalian ENTs and producing sufficient concentrations of protein (up to 10 mg/mL) for future structural studies (Lacapère et al. 2007). This approach can be scaled up and uses a *lac* promoter to drive expression plus tandem affinity purification to isolate N-HAT-3×FLAG-hENT1. N-HAT-3×FLAG-hENT1 differs from endogenous ENT1 by the addition of tandem N-terminal tags (HAT and 3×FLAG) for purification and by the lack of glycosylation (Fig. 1). Initially, Coomassie blue stained gels could not be used to confirm the presence of N-HAT-3×FLAG-hENT1 in lysates because of low expression levels (Fig. 2A). However, anti-3×FLAG immunoblots (Fig. 2B) clearly displayed evidence of N-HAT-3×FLAG-hENT1 expression as a broad band at approximately 47 kDa, slightly lower than the sequence-based expected molecular weight of 57 kDa. This difference is not surprising, since higher mobility shifts are a common characteristic of integral membrane proteins, probably because of their hydrophobicity (Tate et al. 2003; Christoffers et al. 2005; Geyer et al. 2007). Nevertheless, the size of N-HAT-3×FLAG-hENT1 fits well within the reported range for endogenous hENT1, 37–55 kDa (Kwong et al. 1988, 1992, 1993) (the size varies owing to differential glycosylation; Kwong et al. 1986). Furthermore, the observed protein size is remarkably similar to that of recombinant hENT1 overexpressed in mammalian, insect, and yeast hosts (Vickers et al. 1999; Reyes et al. 2010; Ward et al. 2000; G. Reyes and I.R. Coe, unpublished data).

In addition to the apparent full-length N-HAT-3×FLAG-hENT1, 3 additional immunoreactive protein species were

Fig. 1. Putative topological model of N-HAT-3×FLAG-hENT1 overexpressed in *E. coli*. Expressed N-HAT-3×FLAG-hENT1 is theoretically inserted in the inner membrane and putatively composed of 11 transmembrane domains with one large loop facing the periplasmic space and the other large loop facing the cytoplasm. N-HAT-3×FLAG-hENT1 is likely non-glycosylated at Asn48 and has two tandem tags, HAT (circles with X) and 3×FLAG (filled circles), for optimal purification.
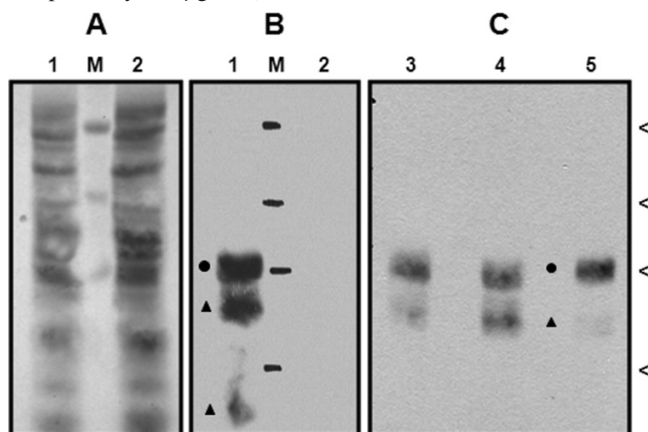

observed. Protein bands smaller than 47 and 32 kDa may be degradation or truncation products (Fig. 2B), while a much larger protein species above 83 kDa could be a dimeric form of N-HAT-3×FLAG-hENT1 (see Fig. 4). To determine whether the two smaller protein species resulted from degradation or truncation, cultures were incubated at lower temperatures. Anti-3×FLAG immunodetection (Fig. 2C) revealed that temperature does affect expression of N-HAT-3×FLAG-hENT1. There appears to be a threshold temperature (<25 °C) favoring expression of full-length and putative dimer protein species (Fig. 2C, lane 5; note that the dimer is visible only with longer film exposures and is not shown here). Below this threshold (i.e., 20 °C), the existence of degradation or truncation by-products is reduced. This is a common phenomenon observed with overexpression of both cytoplasmic and membrane proteins in *E. coli* (Schein and Noteborn 1988; Quick and Wright 2002; Tate et al. 2003; Dyson et al. 2004) and is attributed to the general slowing down of the transcriptional and translational machinery of the host, which allows more time for proteins to be properly synthesized (Baneyx and Mujacic 2004). Lower incubation temperatures also reduce protease activity, which is believed to be up-regulated as a natural response by the host to counteract increasing levels of toxic foreign protein (Enfors 1992; Baneyx and Mujacic 2004).

The larger protein species (>83 kDa) was more apparent in purified fractions and its presence was inconsistent during repeated experiments. Interestingly, this feature of hENT1

has been observed since the late 1980s (at this time known as band 4.5; Jarvis et al. 1986; Jhun et al. 1990) and in a more recent study (Ward et al. 2000), yet no further studies of the nature of this protein species have been done, and the physiological relevance of the putative dimers remains unclear. The same observation was made following overexpression of ENT1 in mammalian and yeast systems (Vickers et al. 1999; Reyes et al. 2010), but it is currently unknown whether this protein species is an artefact of overexpression or represents a physiologically relevant protein complex. Trafficking of some membrane proteins in eukaryotic cells from the endoplasmic reticulum, and other vesicular compartments, has been shown to involve oligomerization of the membrane protein (Sitte et al. 2004). Also, transporters have been discovered to naturally form oligomers in the plasma membrane (i.e., hOAT1, hGlyT, hMDRP1; Hong et al. 2005; Yang et al. 2007; Bartholomäus et al. 2008). Combining these observations with reports on the regulation of transporters through dimerization (Yang et al. 2007) and observations that strong bonds in dimers can withstand the denaturing conditions of SDS–PAGE (i.e., β2-adrenergic receptor; Salahpour et al. 2003), we believe that it is highly likely that hENT1 dimerizes and the potential physiological relevance of this regulatory mechanism warrants further investigation.

Overall, the success of the expression system described here is primarily attributed to identifying the correct promoter

Fig. 2. Immunoblots confirm the overexpression of N-HAT-3×FLAG-hENT1 in *E. coli*. (A) Coomassie blue stained gels revealed no differences between lysates of pN-HAT-3×FLAG-hENT1 transformed cells and non-transformed controls (lanes 1 and 2, respectively; 90 µg total protein). (B) Anti-3×FLAG immunodetection demonstrated that N-HAT-3×FLAG-hENT1 was present in lysates derived from transformed bacterial cells (lane 1) compared with controls (lane 2). Three immunoreactive protein species were detected: full-length protein (∼47 kDa, ●) and two degraded or truncated versions of the protein (<47 and <32 kDa, ▲). Lane M contains the protein markers (<; 83, 62, 47, and 32 kDa). (C) Anti-3×FLAG immunoblot of crude bacterial cell lysates from transformed bacteria grown at 37 °C, 25 °C, and 20 °C (lanes 3, 4, and 5, respectively; 50 µg/lane).

Fig. 3. NBTI binding assays confirm N-HAT-3×FLAG-hENT1 overexpression in *E. coli* and suggest proper conformation. NBTI binding assays were conducted on whole N-HAT-3×FLAG-hENT1 transformed (BFh) and control bacterial cells that were untreated or osmotically shocked (O.S.). These assays demonstrate that bacterial cells are expressing N-HAT-3×FLAG-hENT1, as there is greater NBTI binding (3.2-fold) in transformed cells than in controls. Moreover, NBTI binding is observed only in transformed cells that are osmotically shocked. This is a representative figure from three trials. Anti-3×FLAG immunodetection shows the presence of N-HAT-3×FLAG-hENT1 (arrow) within inner-membrane fractions (inset, IM, 50 µg/lane). Markers (<) are 83, 62, and 47 kDa.
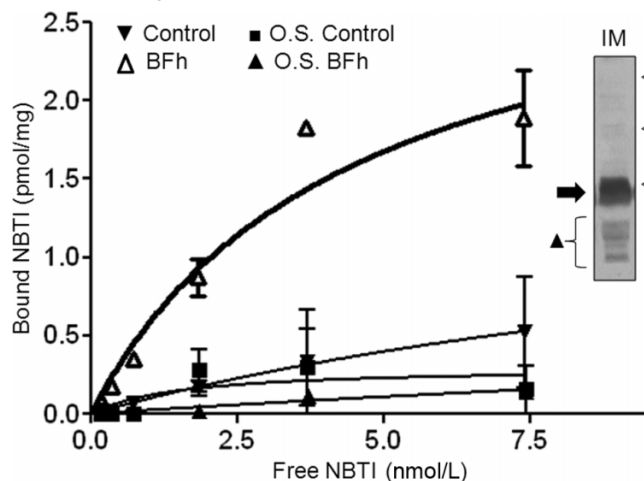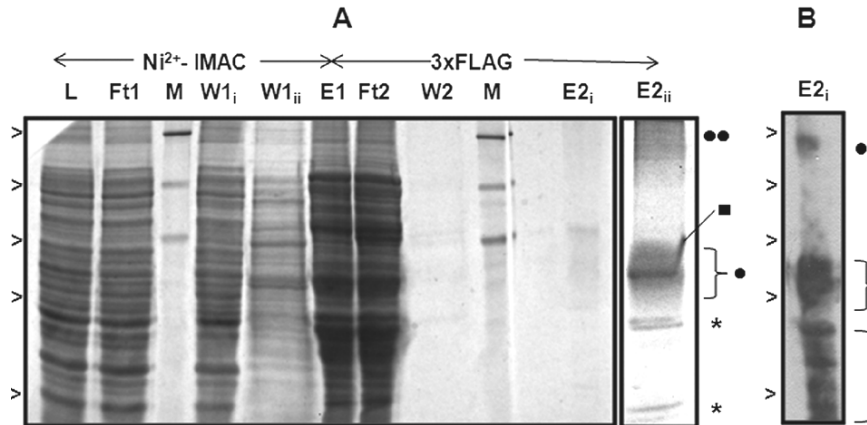

for expression of N-HAT-3×FLAG-hENT1. We found, as have others (Quick and Wright 2002; Tate et al. 2003), that inducible T7 promoters are not always optimal for expression of IMPs, since protein production by these promoters can overwhelm the translational capacity of the host. This results in the accumulation of toxic mRNA levels that promote cell death (Miroux and Walker 1996) and high levels of truncated or misfolded proteins, which promote protease activity (Baneyx and Mujacic 2004). In contrast, the use of a *lac* promoter in the expression construct allowed for a slow constitutive transcription rate that was well tolerated by the translational machinery of the bacterial host. The tolerance for membrane protein overexpression by the highly acclaimed specialized *E. coli* BL21(DE3) strains C41 and C43 follows this mechanism, but the reduced transcription rate results from mutation(s) affecting the *lac* promoter governing the T7 RNA polymerase (Wagner et al. 2008). This approach was also adopted in the successful overexpression of bacterial PutP and the human Na⁺/glucose cotransporter hSGLT1 (Quick and Jung 1998; Quick and Wright 2002).

N-HAT-3×FLAG-hENT1 conformation

To test whether N-HAT-3×FLAG-hENT1 has proper ligand-binding conformation, NBTI binding assays were conducted (Fig. 3). A 3.2-fold increase in NBTI binding was observed between osmotically shocked transformed bacterial cells and controls (B_{max}: ENT1, 1.49 ± 0.39 pmol/mg; control, 0.47 ± 0.31 pmol/mg; $n = 3$), while affinity for NBTI binding was in the nanomolar range (K_d, 10.45 ± 4.51 nmol/L; $n = 3$). These data not only support the conclu-

sion that N-HAT-3×FLAG-hENT1 is expressed in bacteria, explaining the increase in NBTI binding, but also suggest that N-HAT-3×FLAG-hENT1 has been processed and folded in a conformation capable of binding ligand. It is believed that N-HAT-3×FLAG-hENT1 is inserted into the inner membrane, since NBTI binding was observed only in transformed bacterial cells that were osmotically shocked, which renders the outer membrane of the bacterial cell porous to NBTI (Fig. 3). Also, anti-3×FLAG immunodetection confirmed the presence of N-HAT-3×FLAG-hENT1 in isolated inner-membrane fractions (Fig. 3, inset). While it remains a possibility, we do not believe that NBTI is binding to N-HAT-3×FLAG-hENT1 deposited within the cell in inclusion bodies, since the shocked bacterial cells have inner membranes that are fully sealed, which was confirmed through cell viability tests after osmotic shock treatment (data not shown).

N-HAT-3×FLAG-hENT1 NBTI binding (B_{max}) and affinity (K_d) appear to be lower than those observed for some endogenous ENT1 and for recombinant ENT1 expressed in eukaryotic cells (Boumah et al. 1992; Vickers et al. 1999; Reyes et al. 2010). The total amount of ENT1 inserted into the inner membrane (or possibly into inclusion bodies) may be affected by the unnatural lipid environment of the protein (as noted with overexpression of hSGLT1 in bacteria; Quick and Wright 2002). N-HAT-3×FLAG-hENT1 is not N-glycosylated, and likely also not O-glycosylated, since these posttranslational modifications are absent or restricted to certain endogenous proteins in the *E. coli* strain (Wacker et al. 2002; Charbonneau and Mourez 2008). Studies in which hENT1 was overexpressed in yeast suggest that the

Fig. 4. Tandem purification of N-HAT-3×FLAG-hENT1. Aliquots from the various steps of the N-HAT-3×FLAG-hENT1 purification from large-volume trials were analyzed with (A) Coomassie blue stained gels and (B) anti-3×FLAG immunodetection (40 s exposure). Ni^{2+}-IMAC (immobilized-metal affinity chromatography) lanes: L, total solubilized cell lysate (80 µg); Ft1, flow-through (80 µg); $W1_i$ and $W1_{ii}$, washes (80 and 40 µg); E1, eluate (80 µg). 3×FLAG lanes: Ft2, flow-through (80 µg); W2, washes (2 µg); $E2_i$ and $E2_{ii}$, eluate (4 and 40 µg). On Coomassie blue stained gels, N-HAT-3×FLAG-hENT1 (●) and its putative dimer (●●) were detectable only in the 3×FLAG-purified elution fraction (lanes $E2_i$ and $E2_{ii}$). Other minor bands observed in this elution fraction are heavy-chain IgG (■) and some unknown nonspecifically bound proteins (*). N-HAT-3×FLAG-hENT1 and its putative dimer were also confirmed on immunoblots (B) along with some minor degradation or truncation products (▲) that are not detectable on Coomassie blue stained gels. Lanes M contain the protein markers (>; 175, 83, 62, 47, and 32 kDa).

lack of this posttranslational modification on ENT1 affects NBTI binding only and not substrate binding or drug sensitivity (Vickers et al. 1999), which likely explains the lower affinity for NBTI binding observed here than typically observed with endogenous ENT1 or recombinant ENT1 expressed in eukaryotic cells ($K_d \approx 0.1$–0.3 nmol/L) (e.g., Boumah et al. 1992; Vickers et al. 1999; Reyes et al. 2010). However, NBTI binding in the nanomolar range still suggests a high affinity for the expressed protein, supporting our contention that the protein is in the correct conformation.
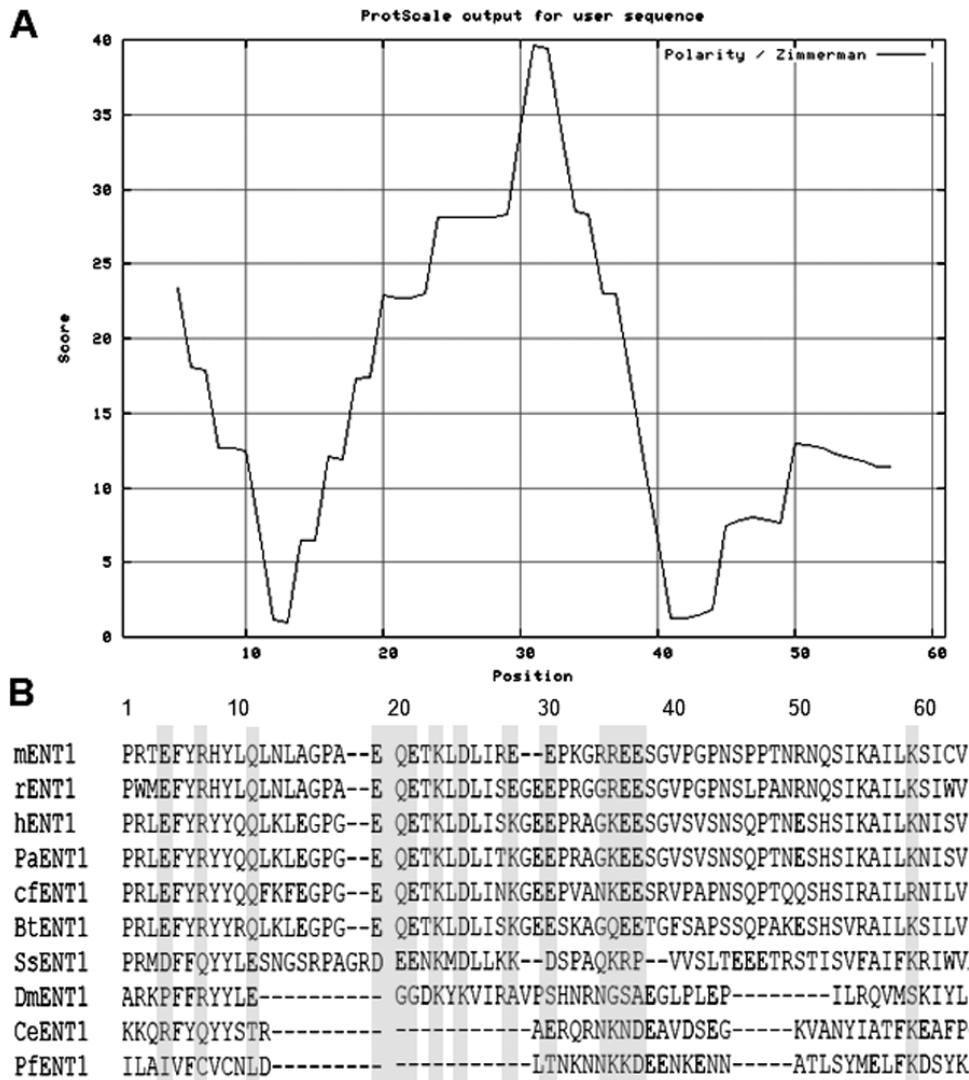
Tandem affinity purification

Having confirmed the expression of N-HAT-3×FLAG-hENT1 and checked its ligand binding characteristics, we then proceeded with its tandem purification. From 1 L fermentor cultures, approximately 15 µg of N-HAT-3×FLAG-hENT1 was purified. This yield ($\sim$15 µg/L of culture) of recombinant membrane protein is lower than values obtained from other similar studies (i.e., FLAG-tagged hSGLT1, 3 mg/L; 6×His-tagged hSERT, 3 mg/L; 6×His-tagged rOAT3, 300 µg/L; Quick and Wright 2002; Tate et al. 2003; Lash et al. 2007), but as a prototypic method this approach provides the largest source of conformationally intact hENT1 in a format that can be extracted easily, thus validating further efforts to refine the process in the future. Currently, extraction of endogenous and recombinant ENT1 from mammalian sources is hampered by the lack of suitable antibodies for immunoprecipitation; also, extraction of recombinant ENT1 from mammalian sources is not economically practical owing to the smaller yields. However, these low yields can be offset by using larger fermentors or by pooling various batches.

Purified N-HAT-3×FLAG-hENT1 was clearly detected on Coomassie blue stained gels and anti-3×FLAG immunoblots (Figs. 4A and 4B). Other protein bands that were observed in the final elution fraction were putative dimers of N-HAT-3×FLAG-hENT1 and minor degradation or truncation products that were visible only through immunodetection. Contaminants from the elution procedure, such as heavy and light chains of IgG (50 kDa and 25 kDa) and some nonspecifically bound proteins, were also observed. Our experiences purifying recombinant ENT1 peptides from *E. coli* and recombinant full-length ENT1 protein from mammalian cells (Reyes et al. 2010) suggest that these contaminating proteins can be removed by alternative elution procedures such as the use of 3×FLAG-peptides, low pH solution, or gel filtration chromatography.

The advantage of the bacterial overexpression protocol described here is that it allows overexpression of the full-length ENT1 protein. While it is possible to investigate smaller regions of membrane proteins, particularly the regions that are cytosolic such as N- or C-termini and intracellular loops, for ENT1 there is limited opportunity to investigate structural aspects of the protein using this approach, since the N-terminus is very short, the C-terminus is extracellular, and all but one of the intracellular loops are very short. The longest intracellular loop in mammalian ENT1 is between transmembrane domains 6 and 7 (Fig. 1) and is predicted to be approximately 60 amino acids in length. This region has potential consensus sites for phosphorylation by kinases (in both mENT1 and hENT1) and thus may contribute to important regulatory interactions with other proteins. Protein prediction programs such as PSIPRED predict a helical structure at the beginning of the intracellular loop, while other regions are predicted to be strands, short helices, or unstructured (Fig. 5A). We tested this prediction by overexpressing, and analyzing by NMR spectroscopy, the hENT1 and mENT1 TM6–TM7 loop (tagged with ubiquitin) using a spectrum of ubiquitin–PirB, which consists of a small random coil fused to ubiquitin, as a control (Figs. 5B and 5C). Analysis of the ENT1 loop

Fig. 5. Large intracellular loop of ENT1 is unstructured based on comparative NMR analysis. (A) Computationally derived predicted secondary structures present in the 61 residue large intracellular loop of human ENT1. The structure primarily consists of short helices at the beginning and end of the input sequences. (B) Coomassie blue stained gel loaded with gel filtration chromatography purified Ubq–hENT1 and Ubq–mENT1 (lane 1 and lane 2, 10 μg/lane). Marker bands shown are 32, 25, 16, and 6 kDa. (C) NMR spectrum of Ubq–PirB (control) and Ubq–ENT1 (Ubq–ENT1 is a representative spectrum of hENT1 and mENT1, since these were identical). The large intracellular loop of ENT1 lacks secondary structure, since its spectrum is almost identical to that of the unstructured control (Ubq–PirB).

(both mouse and human) suggested this region of the protein is predominantly unstructured in solution. This result, however, does not rule out the possibility that this segment is involved in protein–protein interactions, since there are distinct levels of polarity within this segment that result from charged residues which are highly conserved within different organisms (Fig. 6). Moreover, previous studies have provided evidence that an electrostatic cloud produced on a disordered extra- or intracellular loop, as we have identified in ENT1, can serve as a dynamic regulatory domain sensitive to conformational changes (Conseil et al. 2009; Fusca et al. 2009). Furthermore, similar domains can serve as binding sites to attract associating proteins such as kinases (Mittag et al. 2010; Galdiero et al. 2003). Direct phos-

phorylation of a transporter by kinases may be a regulatory mechanism, although, to date, this has not been demonstrated for any nucleoside transporter.

Conclusion

In this report we present the first bacterial expression of a mammalian equilibrative nucleoside transporter. By using a construct driven by a *lac* promoter and isolation through tandem affinity purification techniques, we were able to isolate conformationally correct N-HAT-3×FLAG-hENT1 at a concentration of approximately 15 μg/L of culture, demonstrating that this approach is feasible and can be used to obtain sufficient amounts of protein for further structural analysis. Analysis of the large intracellular loop between transmem-

Fig. 6. The unstructured large intracellular loop of ENT1 possesses high degrees of conserved polarity. (A) Predicted polar regions contained within the large intracellular loop of mENT1 determined with ProtScale (Zimmerman amino acid scale). (B) Sequence alignment of large ENT1 intracellular loop with ClustalW shows that these polar regions result from highly conserved charged residues (e.g., E, D, R, K, Q). ENT1 sequences from a variety of organisms, representing a broad range of taxa, were aligned for comparison: mouse (mENT1, GI:8698616), rat (rENT1, GI:5092794), human (hENT1, GI:1845344), orangutan (PaENT1, GI:229576941), canine (cfENT1, GI:50979327), bovine (BtENT1, GI:296474415), salmon (SsENT1, GI223649482), *D. melanogaster* (DmENT1, GI:24580624), *C. elegans* (CeENT1, GI:21311330), and *Plasmodium falciparum* (PfENT1, GI:9963825).

brane domains 6 and 7 suggests that this loop exists in a predominantly unstructured state. Our results present a novel but prototypic source of hENT1 for structural studies, which can lead to the development of three-dimensional models to provide insight into the substrate binding and transport mechanisms of this clinically important integral membrane protein.

Acknowledgements

References

Baneyx, F., and Mujacic, M. 2004. Recombinant protein folding and misfolding in *Escherichia coli.* Nat. Biotechnol. **22**(11): 1399–1408. doi:10.1038/nbt1029. PMID:15529165.

Bartholomäus, I., Milan-Lobo, L., Nicke, A., Dutertre, S., Hastrup, H., Jha, A., et al. 2008. Glycine transporter dimers: evidence for occurrence in the plasma membrane. J. Biol. Chem. **283**(16): 10978–10991. doi:10.1074/jbc.M800622200. PMID:18252709.

Blundell, T.L., Sibanda, B.L., Montalvão, R.W., Brewerton, S., Chelliah, V., Worth, C.L., et al. 2006. Structural biology and bioinformatics in drug design: opportunities and challenges for target identification and lead discovery. Philos. Trans. R. Soc.

Lond. B Biol. Sci. **361**(1467): 413–423. doi:10.1098/rstb.2005. 1800. PMID:16524830.

Boumah, C.E., Hogue, D.L., and Cass, C.E. 1992. Expression of high levels of nitrobenzylthioinosine-sensitive nucleoside transport in cultured human choriocarcinoma (BeWo) cells. Biochem. J. **288**(Pt 3): 987–996. PMID:1472012.

Bryson, K., McGuffin, L.J., Marsden, R.L., Ward, J.J., Sodhi, J.S., and Jones, D.T. 2005. Protein structure prediction servers at University College London. Nucleic Acids Res. **33**(Web Server issue): W36–W38. doi:10.1093/nar/gki410.

Charbonneau, M.E., and Mourez, M. 2008. The *Escherichia coli* AIDA-I autotransporter undergoes cytoplasmic glycosylation independently of export. Res. Microbiol. **159**(7–8): 537–544. doi:10.1016/j.resmic.2008.06.009. PMID:18657609.

Chenna, R., Sugawara, H., Koike, T., Lopez, R., Gibson, T.J., Higgins, D.G., and Thompson, J.D. 2003. Multiple sequence alignment with the Clustal series of programs. Nucleic Acids Res. **31**(13): 3497–3500. PMID:12824352.

Christoffers, K.H., Li, H., and Howells, R.D. 2005. Purification and mass spectrometric analysis of the delta opioid receptor. Brain Res. Mol. Brain Res. **136**(1–2): 54–64. doi:10.1016/j. molbrainres.2005.01.016. PMID:15893587.

Congreve, M., Murray, C.W., and Blundell, T.L. 2005. Structural biology and drug discovery. Drug Discov. Today, **10**(13): 895–907. doi:10.1016/S1359-6446(05)03484-7. PMID:15993809.

Conseil, G., Rothnie, A.J., Deeley, R.G., and Cole, S.P.C. 2009. Multiple roles of charged amino acids in cytoplasmic loop 7 for expression and function of the multidrug and organic anion transporter MRP1 (ABCC1). Mol. Pharmacol. **75**(2): 397–406. doi:10.1124/mol.108.052860. PMID:19015228.

Delaglio, F., Grzesiek, S., Vuister, G.W., Zhu, G., Pfeifer, J., and Bax, A. 1995. NMRPipe: a multidimensional spectral processing system based on UNIX pipes. J. Biomol. NMR, **6**(3): 277–293. doi:10.1007/BF00197809. PMID:8520220.

Dyson, M.R., Shadbolt, S.P., Vincent, K.J., Perera, R.L., and McCafferty, J. 2004. Production of soluble mammalian proteins in *Escherichia coli*: identification of protein features that correlate with successful expression. BMC Biotechnol. **4**(1): 32. doi:10.1186/1472-6750-4-32. PMID:15598350.

Enfors, S.O. 1992. Control of *in vivo* proteolysis in the production of recombinant proteins. Trends Biotechnol. **10**(9): 310–315. doi:10.1016/0167-7799(92)90256-U. PMID:1369412.

Fusca, T., Bonza, M.C., Luoni, L., Meneghelli, S., Marrano, C.A., and De Michelis, M.I. 2009. Single point mutations in the small cytoplasmic loop of ACA8, a plasma membrane Ca^{2+}-ATPase of *Arabidopsis thaliana,* generate partially deregulated pumps. J. Biol. Chem. **284**(45): 30881–30888. doi:10.1074/jbc.M109. 006148. PMID:19740735.

Galdiero, S., Capasso, D., Vitiello, M., D'Isanto, M., Pedone, C., and Galdiero, M. 2003. Role of surface-exposed loops of *Haemophilus influenzae* protein P2 in the mitogen-activated protein kinase cascade. Infect. Immun. **71**(5): 2798–2809. doi:10.1128/ IAI.71.5.2798-2809.2003. PMID:12704154.

Gasteiger, E., Hoogland, C., Gattiker, A., Duvaud, S., Wilkins, M.R., Appel, R.D., and Bairoch. A. Protein identification and analysis tools on the ExPASy server. *In* The proteomics protocols handbook. *Edited by* J.M. Walker. Humana Press, Totowa, N.J. pp. 571–607.

Geyer, J., Döring, B., Meerkamp, K., Ugele, B., Bakhiya, N., Fernandes, C.F., et al. 2007. Cloning and functional characterization of human sodium-dependent organic anion transporter (SLC10A6). J. Biol. Chem. **282**(27): 19728–19741. doi:10.1074/ jbc.M702663200. PMID:17491011.

Granseth, E., Seppälä, S., Rapp, M., Daley, D.O., and Von Heijne,

G. 2007. Membrane protein structural biology — how far can the bugs take us? Mol. Membr. Biol. **24**(5–6): 329–332. doi:10. 1080/09687680701413882. PMID:17710636.

Hofmann, K., and Stoffel, W. 1993. TMbase — A database of membrane spanning proteins segments. Biol. Chem. Hoppe Seyler, **374**: 166.

Hong, M., Xu, W., Yoshida, T., Tanaka, K., Wolff, D.J., Zhou, F., et al. 2005. Human organic anion transporter hOAT1 forms homooligomers. J. Biol. Chem. **280**(37): 32285–32290. doi:10. 1074/jbc.M501447200. PMID:16046403.

Jarvis, S.M., Ellory, J.C., and Young, J.D. 1986. Radiation inactivation of the human erythrocyte nucleoside and glucose transporters. Biochim. Biophys. Acta, **855**(2): 312–315. doi:10.1016/ 0005-2736(86)90179-3. PMID:3947628.

Jhun, B.H., Rampal, A.L., Berenski, C.J., and Jung, C.Y. 1990. Chromatographic characterization of nitrobenzylthioinosine binding proteins in band 4.5 of human erythrocytes: purification of a 40 kDa truncated nucleoside transporter. Biochim. Biophys. Acta, **1028**(3): 251–260. doi:10.1016/0005-2736(90)90174-M. PMID:2223799.

Johnson, B.A., and Blevins, R.A. 1994. NMR View: a computer program for the visualization and analysis of NMR data. J. Biomol. NMR, **4**(5): 603–614. doi:10.1007/BF00404272.

King, A.E., Ackley, M.A., Cass, C.E., Young, J.D., and Baldwin, S.A. 2006. Nucleoside transporters: from scavengers to novel therapeutic targets. Trends Pharmacol. Sci. **27**(8): 416–425. doi:10.1016/j.tips.2006.06.004. PMID:16820221.

Kotarski, S.F., and Salyers, A.A. 1984. Isolation and characterization of outer membranes of *Bacteroides thetaiotaomicron* grown on different carbohydrates. J. Bacteriol. **158**(1): 102–109. PMID: 6715279.

Kwong, F.Y., Baldwin, S.A., Scudder, P.R., Jarvis, S.M., Choy, M.Y., and Young, J.D. 1986. Erythrocyte nucleoside and sugar transport. Endo-β-galactosidase and endoglycosidase-F digestion of partially purified human and pig transporter proteins. Biochem. J. **240**(2): 349–356. PMID:3101670.

Kwong, F.Y., Davies, A., Tse, C.M., Young, J.D., Henderson, P.J., and Baldwin, S.A. 1988. Purification of the human erythrocyte nucleoside transporter by immunoaffinity chromatography. Biochem. J. **255**(1): 243–249. PMID:3196318.

Kwong, F.Y., Fincham, H.E., Davies, A., Beaumont, N., Henderson, P.J., Young, J.D., and Baldwin, S.A. 1992. Mammalian nitrobenzylthioinosine-sensitive nucleoside transport proteins. Immunological evidence that transporters differing in size and inhibitor specificity share sequence homology. J. Biol. Chem. **267**(30): 21954–21960. PMID:1400505.

Kwong, F.Y., Wu, J.S., Shi, M.M., Fincham, H.E., Davies, A., Henderson, P.J., et al. 1993. Enzymic cleavage as a probe of the molecular structures of mammalian equilibrative nucleoside transporters. J. Biol. Chem. **268**(29): 22127–22134. PMID: 8408072.

Lacapère, J.J., Pebay-Peyroula, E., Neumann, J.M., and Etchebest, C. 2007. Determining membrane protein structures: still a challenge! Trends Biochem. Sci. **32**(6): 259–270. doi:10.1016/j.tibs. 2007.04.001. PMID:17481903.

Lash, L.H., Putt, D.A., Xu, F., and Matherly, L.H. 2007. Role of rat organic anion transporter 3 (Oat3) in the renal basolateral transport of glutathione. Chem. Biol. Interact. **170**(2): 124–134. doi:10.1016/j.cbi.2007.07.004. PMID:17719021.

Löffler, M., Morote-Garcia, J.C., Eltzschig, S.A., Coe, I.R., and Eltzschig, H.K. 2007. Physiological roles of vascular nucleoside transporters. Arterioscler. Thromb. Vasc. Biol. **27**(5): 1004–1013. doi:10.1161/ATVBAHA.106.126714. PMID:17332491.

Miroux, B., and Walker, J.E. 1996. Over-production of proteins in

Escherichia coli: mutant hosts that allow synthesis of some membrane proteins and globular proteins at high levels. J. Mol. Biol. **260**(3): 289–298. doi:10.1006/jmbi.1996.0399. PMID: 8757792.

Mittag, T., Kay, L.E., and Forman-Kay, J.D. 2010. Protein dynamics and conformational disorder in molecular recognition. J. Mol. Recognit. **23**(2): 105–116. PMID:19585546.

Neu, H.C., and Heppel, L.A. 1965. The release of enzymes from *Escherichia coli* by osmotic shock and during the formation of spheroplasts. J. Biol. Chem. **240**(9): 3685–3692. PMID:4284300.

Noji, T., Karasawa, A., and Kusaka, H. 2004. Adenosine uptake inhibitors. Eur. J. Pharmacol. **495**(1): 1–16. doi:10.1016/j.ejphar. 2004.05.003. PMID:15219815.

Quick, M., and Jung, H. 1998. A conserved aspartate residue, Asp187, is important for Na$^+$-dependent proline binding and transport by the Na$^+$/proline transporter of *Escherichia coli*. Biochemistry, **37**(39): 13800–13806. doi:10.1021/bi980562j. PMID: 9753469.

Quick, M., and Wright, E.M. 2002. Employing *Escherichia coli* to functionally express, purify, and characterize a human transporter. Proc. Natl. Acad. Sci. U.S.A. **99**(13): 8597–8601. doi:10. 1073/pnas.132266599. PMID:12077304.

Reithmeier, R.A. 2007. Structural biology of membrane proteins. Methods, **41**(4): 353–354. doi:10.1016/j.ymeth.2007.02.016. PMID:17367708.

Reyes, G., Naydenova, Z., Abdulla, P., Chalsev, M., Villani, A., Rose, J.B., et al. 2010. Characterization of mammalian equilibrative nucleoside transporters (ENTs) by mass spectrometry. Protein Expr. Purif. **73**(1): 1–9. doi:10.1016/j.pep.2010.04.008. PMID:20399865.

Rose, J.B., and Coe, I.R. 2008. Physiology of nucleoside transporters: back to the future.... Physiology (Bethesda), **23**: 41–48. PMID:18268364.

Salahpour, A., Bonin, H., Bhalla, S., Petäjä-Repo, U., and Bouvier, M. 2003. Biochemical characterization of β2-adrenergic receptor dimers and oligomers. Biol. Chem. **384**(1): 117–123. doi:10. 1515/BC.2003.012. PMID:12674505.

Schein, C.H., and Noteborn, N.H.M. 1988. Formation of soluble recombinant proteins in *Escherichia coli* is favored by lower growth temperatures. Biotechnology (N.Y.), **6**(3): 291–294. doi:10.1038/nbt0388-291.

Sitte, H.H., Farhan, H., and Javitch, J.A. 2004. Sodium-dependent neurotransmitter transporters: oligomerization as a determinant of transporter function and trafficking. Mol. Interv. **4**(1): 38–47. doi:10.1124/mi.4.1.38. PMID:14993475.

Tate, C.G., Haase, J., Baker, C., Boorsma, M., Magnani, F., Vallis, Y., and Williams, D.C. 2003. Comparison of seven different heterologous protein expression systems for the production of the serotonin transporter. Biochim. Biophys. Acta, **1610**(1): 141–153. doi:10.1016/S0005-2736(02)00719-8. PMID:12586388.

Vickers, M.F., Mani, R.S., Sundaram, M., Hogue, D.L., Young, J.D., Baldwin, S.A., and Cass, C.E. 1999. Functional production and reconstitution of the human equilibrative nucleoside transporter (hENT1) in *Saccharomyces cerevisiae*. Interaction of inhibitors of nucleoside transport with recombinant hENT1 and a glycosylation-defective derivative (hENT1/N48Q). Biochem. J. **339**(1): 21–32. doi:10.1042/0264-6021:3390021. PMID: 10085223.

Wacker, M., Linton, D., Hitchen, P.G., Nita-Lazar, M., Haslam, S.M., North, S.J., et al. 2002. N-linked glycosylation in *Campylobacter jejuni* and its functional transfer into *E. coli*. Science, **298**(5599): 1790–1793. doi:10.1126/science.298.5599.1790. PMID:12459590.

Wagner, S., Klepsch, M.M., Schlegel, S., Appel, A., Draheim, R., Tarry, M., et al. 2008. Tuning *Escherichia coli* for membrane protein overexpression. Proc. Natl. Acad. Sci. U.S.A. **105**(38): 14371–14376. doi:10.1073/pnas.0804090105. PMID:18796603.

Ward, J.L., Sherali, A., Mo, Z.P., and Tse, C.M. 2000. Kinetic and pharmacological properties of cloned human equilibrative nucleoside transporters, ENT1 and ENT2, stably expressed in nucleoside transporter-deficient PK15 cells. Ent2 exhibits a low affinity for guanosine and cytidine but a high affinity for inosine. J. Biol. Chem. **275**(12): 8375–8381. doi:10.1074/jbc.275. 12.8375. PMID:10722669.

Yang, Y., Liu, Y., Dong, Z., Xu, J., Peng, H., Liu, Z., and Zhang, J.T. 2007. Regulation of function by dimerization through the amino-terminal membrane-spanning domain of human ABCC1/ MRP1. J. Biol. Chem. **282**(12): 8821–8830. doi:10.1074/jbc. M700152200. PMID:17264072.

Young, J.D., Yao, S.Y., Sun, L., Cass, C.E., and Baldwin, S.A. 2008. Human equilibrative nucleoside transporter (ENT) family of nucleoside and nucleobase transporter proteins. Xenobiotica, **38**(7–8): 995–1021. doi:10.1080/00498250801927427. PMID: 18668437.